Electronic structure calculations for layered $LaSrMnO_4$ and Ca_2RuO_4

2001 J. Phys.: Condens. Matter 13 9231

(http://iopscience.iop.org/0953-8984/13/41/313)

INSTITUTE OF PHYSICS PUBLISHING JOURNAL OF PHYSICS: CONDENSED MATTER

J. Phys.: Condens. Matter **13** (2001) 9231–9244 PII: S0953-8984(01)21598-7

Electronic structure calculations for layered $LaSrMnO_4$ and Ca_2RuO_4

Key Taeck Park

Department of Physics, Kookmin University, Seoul 136-702, Korea

Received 1 February 2001, in final form 17 April 2001
Published 28 September 2001
Online at stacks.iop.org/JPhysCM/13/9231

Abstract

The electronic structures and magnetic properties of layered perovskite $LaSrMnO_4$ and Ca_2RuO_4 have been determined using the full-potential linearized augmented-plane-wave method within the local spin-density approximation (LSDA) and the LDA + U approach (LDA standing for local density approximation). The results of LSDA and LDA + U total-energy calculations show that the antiferromagnetic state of these materials is stable compared with the ferromagnetic and paramagnetic states. The LDA + U calculation results show that Jahn–Teller distortion of Mn–O and Ru–O octahedra produces an energy gap, and $3z^2 - r^2$ and xy orbital ordering for $LaSrMnO_4$ and Ca_2RuO_4, respectively. However, the LSDA calculation is not sufficient for describing the orbital ordering and fails to produce the band gap. The Jahn–Teller distortion stabilizes a two-dimensional planar antiferromagnetic state.

1. Introduction

Recently, Mn and Ru oxide compounds have been extensively studied, since these compounds with the perovskite structure show a variety of physical properties (superconductivity, colossal magnetoresistance (CMR), magnetic phase transitions etc) [1].

It is well known that the mother material of CMR manganites, $LaMnO_3$, presents A-type antiferromagnetic (AF) insulating behaviour and the Mn^{3+} ($t_{2g}^3 e_g^1$ occupation) causes Jahn–Teller distortion. Similarly, $LaSrMnO_4$ with two-dimensional layered structure also shows AF insulating behaviour and Jahn–Teller distortion. However, the Mn–O plane of $LaSrMnO_4$ exhibits AF structure, while three-dimensional $LaMnO_3$ shows in-plane ferromagnetic (FM) structure. The difference in magnetic structure is closely related to the Jahn–Teller distortion of the two structures.

In the 4d ruthenate case, several magnetic behaviours are presented. $SrRuO_3$ and $CaRuO_3$, which have the same 4d-electron occupations (Ru^{4+}), are three-dimensional FM metals ($T_c = 160$ K) and paramagnetic (PM) metals, respectively. Two-dimensional Sr_2RuO_4

0953-8984/01/419231+14$30.00

with the K_2NiF_4 structure is superconducting below 1.5 K [2]. However, two-dimensional Ca_2RuO_4 with a small degree of Ca-ion substitution is an AF insulator [3, 4]. The magnetism of 4d ruthenate strongly depends on the cation size and dimensionality [4, 5].

It is well known that Jahn–Teller distortion is closely related to the orbital ordering and magnetic ordering. The strength of hybridization and exchange splitting between 3d transition metal and oxide atoms are quite different from those between 4d transition metal and oxide atoms. This leads to there being some differences in orbital ordering, magnetic structure and Jahn–Teller distortion between $LaSrMnO_4$ and Ca_2RuO_4.

In this paper, we focus on the following questions.

(1) The LSDA seems to be sufficient for describing the opening of a band gap in three-dimensional $LaMnO_3$ if the cooperative Jahn–Teller distortion is taken into account. Is it appropriate to expect this for two-dimensional $LaSrMnO_4$ and Ca_2RuO_4?
(2) What are the differences in electronic and magnetic structure between two-dimensional and three-dimensional materials?
(3) Why do 3d ($LaSrMnO_4$) and 4d oxides (Ca_2RuO_4) show different types of Jahn–Teller distortion?
(4) What kinds of orbital ordering exist for $LaSrMnO_4$ and Ca_2RuO_4?

In order to answer the above questions, we performed first-principles LSDA and LDA + U electronic structure calculations for the 3d oxide $LaSrMnO_4$ and the 4d oxide Ca_2RuO_4, which have the same d-band occupations (d^4). We investigated the electronic structure and magnetic structure of both materials and compared our findings with results for three-dimensional materials ($LaMnO_3$ and $SrRuO_3$). Using total-energy calculations for each magnetic configuration (ferromagnetic, antiferromagnetic and paramagnetic states), we studied the magnetic stability.

2. Method

2.1. Crystal structure

$LaSrMnO_4$ has the K_2NiF_4-type body-centred-tetragonal structure (group $I4/mmm$) if spin is not taken into consideration. The K_2NiF_4 crystal structure is shown figure1. Its lattice constants a and c are 3.794 and 13.09 Å, respectively [15]. The spin structure is planar AF and it leads to a doubling of the K_2NiF_4 unit cell ($\sqrt{2}a$, $\sqrt{2}b$, c), while $LaMnO_3$ has the A-type AF structure with an orthorhombic unit cell. The Mn–O–Mn angle is 180° (160° in $LaMnO_3$). The Mn–O octahedron is elongated in the c-direction because of the Jahn–Teller distortion caused by the Mn^{3+} ion. The in-plane distance between Mn and O_1 (1.897 Å) is shorter than the inter-plane Mn–O_2 distance (2.285 Å). This Jahn–Teller distortion is different for three-dimensional $LaMnO_3$, which has Mn–O distances 1.91 and 2.06 Å (the in-plane Mn–O_1 distances) and 1.96 Å (the inter-plane Mn–O_2 distance). These findings are summarized in table 1.

Table 1. The crystal and magnetic structure of Mn and Ru oxides. M is the Mn or Ru atom.

	$LaSrMnO_4$	$LaMnO_3$	Ca_2RuO_4
Structure	Tetragonal	Orthorhombic	Orthorhombic
Phase	AF	AF (A-type)	AF
M–O_2 (Å)	2.285	2.18	2.015, 2.018
M–O_1 (Å)	1.897	1.91, 1.96	1.972

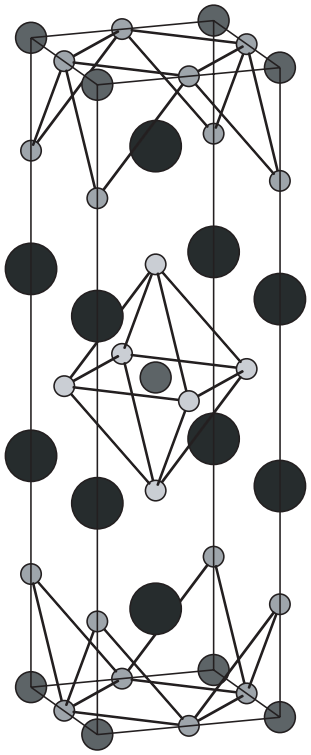

Figure 1. The crystal structure of $LaSrMnO_4$. The black, grey and white spheres represent La or Sr, Mn and O atoms, respectively.

Ca_2RuO_4 has the same K_2NiF_4-type structure as $LaSrMnO_4$. However, the different types of distortion and rotation of the Ru–O octahedron lead to it having orthorhombic structure with *P bca* symmetry [6]. The flattening of RuO_6 octahedron along the *c*-axis is associated with a Jahn–Teller distortion (2.015 and 2.018 Å in-plane Ru–O_1 distances and 1.972 Å inter-plane Ru–O_2 distance). However, the other Ru oxides, Sr_2RuO_4, $CaRuO_3$ and $SrRuO_3$, do not show Jahn–Teller distortion. According to experimental observation, Ca_2RuO_4 is an in-plane AF insulator and Sr_2RuO_4 is a paramagnetic insulator.

2.2. Calculation

For the band-structure and total-energy calculations, we used the self-consistent full-potential linearized augmented-plane-wave (FLAPW) method [14] based on density functional theory [13] within the local spin-density approximation (LSDA) and the LDA + *U* approach. Since non-spherical components are employed for both the potential and the charge density, it is possible to calculate the strong anisotropic interaction in layered materials.

Application of the LSDA approach to transition metal oxide perovskites is quite successful as regards describing the electronic structure for $LaMnO_3$ and Sr_2RuO_4 systems. However, $LaSrMnO_4$ and Ca_2RuO_4 are categorized as Mott insulators. The LSDA approach is not sufficient for describing the insulating behaviour and the orbital ordering. Thus, we employed the LDA + *U* approach. In these calculations, we assumed that $U_{eff} = U - J$ is set to 2.0 eV

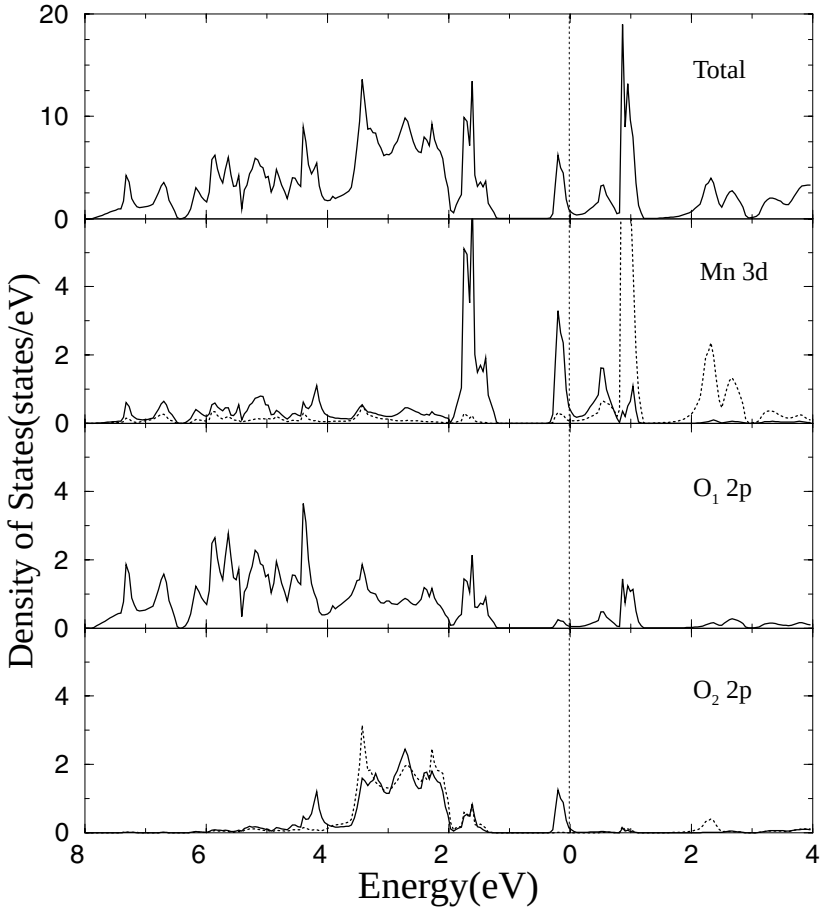

Figure 2. The total density of states and muffin-tin projected partial density of states of $LaSrMnO_4$ obtained by LSDA calculation. Solid and dotted lines in the second and fourth panels represent projected densities of states for up and down spins, respectively.

for Mn 3d and Ru 4d, since we could not find appropriate values of the parameters U and J from experiments.

We treated the 2s and 2p states of O, 3d states of Mn, 4d states of Ru and 5p, 5d and 6s states of La as valence states. The core eigenstates were recomputed in each iteration fully relativistically (i.e. no frozen-core approximation was made). The calculations were made using the Hedin–Lundqvist form of the exchange–correlation potential and the maximum angular momentum quantum number was taken to be $l = 8$ in the expansion of the wave function and in that of the potential. The plane-wave expansion outside the muffin-tin sphere was continued up to $R_{MT}K_{max} = 7.04$. In the self-consistent iterations, 80 tetrahedron k-points are used. Increasing the number of plane waves and mesh k-points did not change the total energy by more than 0.1 mRyd. The muffin-tin radii were chosen to be 3.0 au for La and Ca, 2.0 au for Mn and 1.5 au for O.

In the calculation for $LaSrMnO_4$, we used the virtual-crystal approximation (VCA) for the La and Ba atoms. This approximation does not affect the result, since the La and Sr levels

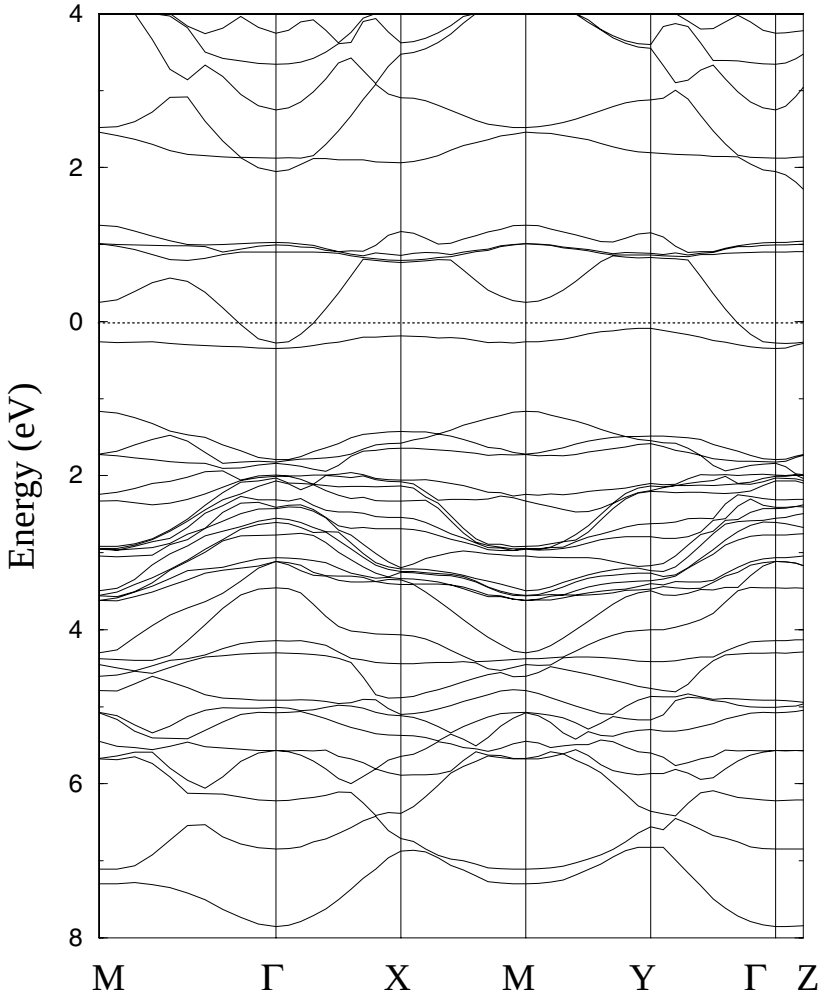

Figure 3. The energy band structure of $LaSrMnO_4$ obtained by LSDA calculation. Γ, X, M, Y and Z represent (0, 0, 0), (1/2, 0, 0), (1/2, 1/2, 0), (0, 1/2, 0), (0, 0, 1) *k*-points in the simple tetragonal Brillouin zone, respectively. The dotted line at 0 eV represents the Fermi level.

are located far from the Fermi level and the La and Sr atoms are not arranged periodically in the experiment.

3. Results and discussion

3.1. $LaSrMnO_4$

Figure 2 shows the calculated total density of states (TDOS) and partial density of states (PDOS) inside muffin-tin spheres for antiferromagnetic $LaSrMnO_4$ based on the LSDA. Because of the high-spin Mn^{3+} ionic states, the up-spin states of t_{2g} are fully occupied and those of Mn e_g are half-filled. Unlike the PDOS of O_1, the PDOS of O_2 represents the localized density of states. The Jahn–Teller distortion (tetragonal distortion of Mn–O octahedra) splits the e_g orbitals into $x^2 - y^2$ and $3z^2 - r^2$ orbitals. The long Mn–O_2 distance

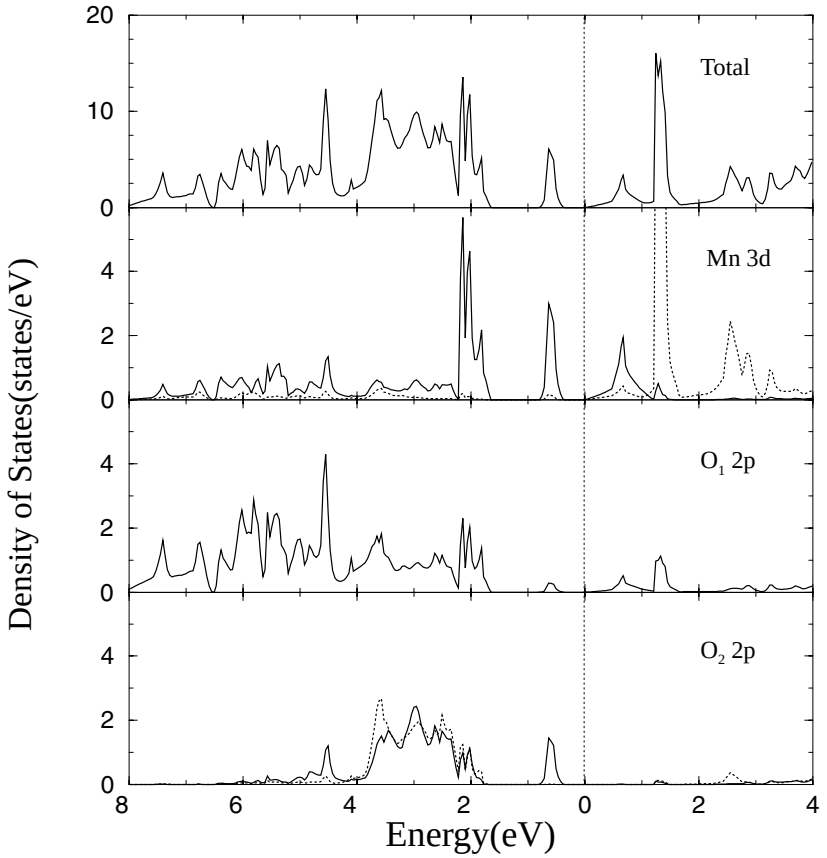

Figure 4. The total density of states and muffin-tin projected partial density of states of $LaSrMnO_4$ obtained by LDA + U calculation. Solid and dotted lines in the second and fourth panels represent projected densities of states for up and down spins, respectively.

and two-dimensionality (non-periodicity along the c-direction) give rise to weak hybridization between Mn $3z^2 - r^2$ and O_2 $2p_z$ orbitals. Thus, this band locates below the $x^2 - y^2$ and O_1 $p_{x,y}$ hybridization band and shows strongly localized character. This band charge density of the (110) plane is shown in figure 3. It represents $3z^2 - r^2$ orbital ordering. Figure 4 shows the LSDA-calculated band structure for the AF state. However, LSDA calculation fails to describe the insulating behaviour of $LaSrMnO_4$ due to Jahn–Teller distortion. Recently, the LDA + U approach to Mott–Hubbard-type insulators has proved quite successful as regards describing the orbital ordering and Jahn–Teller distortion [9, 10]. We employed an LDA + U calculation for $LaSrMnO_4$, which is categorized as a Mott–Hubbard-type strongly electron-correlated material. Figure 5 shows the calculated PDOS and TDOS based on the LDA + U approach. The band gap between $3z^2 - r^2$- and $x^2 - y^2$-related orbitals is about 0.4 eV and this is in good agreement with the optical spectra measurement: 0.55 eV [12]. Figure 6 presents the band structure calculated using the LDA + U approach. It shows the insulating gap, since the $3z^2 - r^2$-orbital-related band lowers and shows more localized behaviour. Even though $LaSrMnO_4$ shows tetragonal symmetry in its crystal structure, the energy of the $3z^2 - r^2$ band is slightly different at the X and Y k-points, because this band is coupled with the other layer. This indicates that magnetic coupling between layers is not negligible in $LaSrMnO_4$.

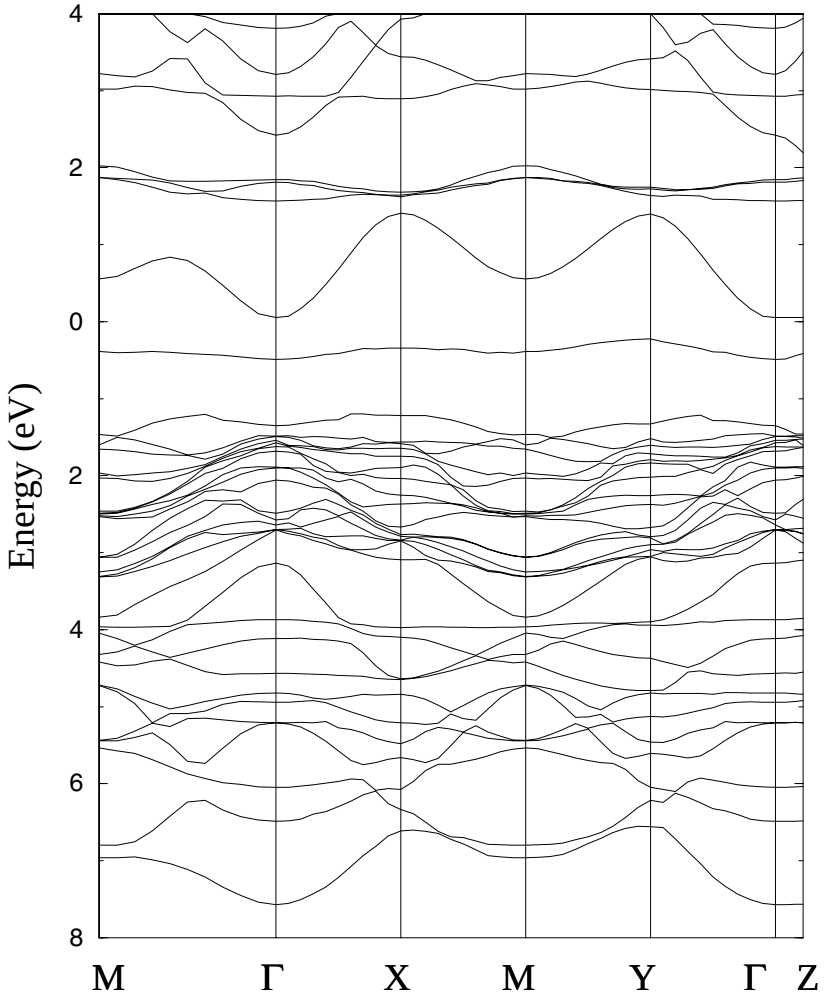

Figure 5. The energy band structure of $LaSrMnO_4$ obtained by LDA + U calculation. Γ, X, M, Y and Z represent (0, 0, 0), (1/2, 0, 0), (1/2, 1/2, 0), (0, 1/2, 0), (0, 0, 1) k-points in the simple tetragonal Brillouin zone, respectively. The conduction band minimum energy is chosen as 0 eV.

However, the $x^2 - y^2$ band (just above 0 eV) is symmetric at these k-points, since this orbital does not couple with those of the other layers.

The calculated magnetic moment inside the muffin-tin spheres is 3.08 and 3.30 μ_B according to the LSDA and LDA + U approaches, respectively. The experimentally observed moment is 0.8 μ_B [7]. This value is quite small compared with that of $LaMnO_3$ ($3.89\mu_B$), which also has Mn^{3+} ions. The small magnetic moment observed from experiments may arise from canted spin structure or helical spin structure of $LaSrMnO_4$. Since this material is very sensitive to the oxygen content [7], we need more accurate experiments.

To investigate the AF stability, we calculated the total energy using the experimental crystal structure within the LSDA. The calculated total energy in the AF state is 28 and 1300 meV/cell

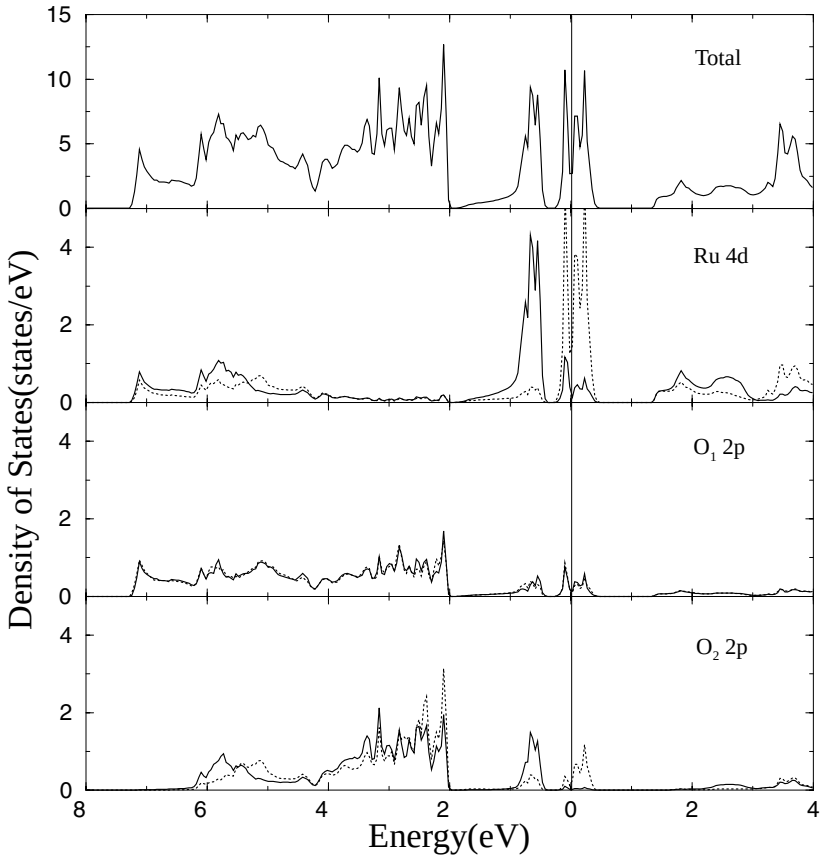

Figure 6. The total density of states and muffin-tin projected partial density of states of Ca_2RuO_4 obtained by LSDA calculation. Solid and dotted lines in the second and fourth panels represent projected densities of states for up and down spins, respectively.

lower than those in the FM and PM states, respectively. According to a simple molecular field approximation with nearest-neighbour interactions, the interaction Hamiltonian is

$$H = -\sum_{j=1}^{4} J(\vec{S}_i \cdot \vec{S}_j). \tag{1}$$

From the above equation, the total energy in the FM state is $E(\mathrm{FM}) = -4JS^2$, while the total energy in the AF state is $E(\mathrm{AF}) = 4JS^2$. Using the FLAPW-calculated energy, we derived the exchange interaction $J = -0.44$ meV. The Néel temperature is given by

$$T_N = \frac{2S(S+1)}{3k_B}(-4J). \tag{2}$$

The calculated Néel temperature is 82 K, which is similar to the experimental value of 180 K. Generally, the calculated Néel temperature is overestimated in the molecular field approximation. The small energy difference between the AF and FM states comes from using the room temperature crystal structure and from the LSDA-related problem of absence of an energy gap. The total-energy differences calculated using the LDA + U approach are 220 meV

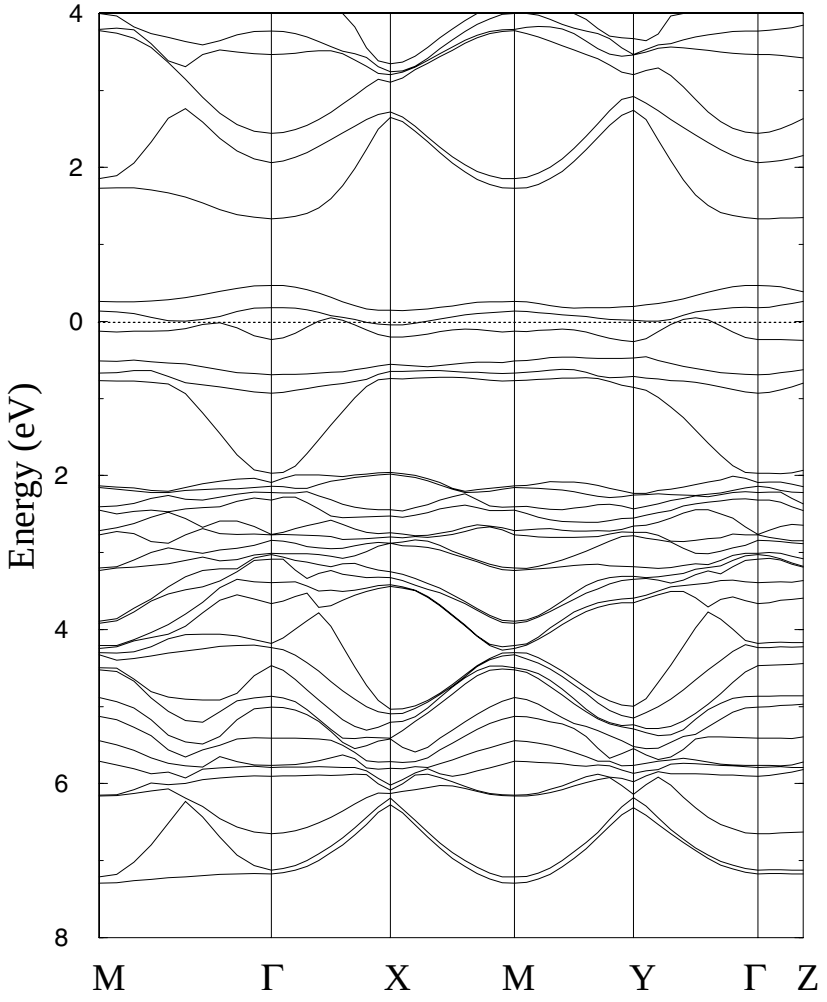

Figure 7. The energy band structure of Ca_2RuO_4 obtained by LSDA calculation. Γ, X, M, Y and Z represent (0, 0, 0), (1/2, 0, 0), (1/2, 1/2, 0), (0, 1/2, 0), (0, 0, 1) *k*-points in the simple orthorhombic Brillouin zone, respectively. The dotted line at 0 eV represents the Fermi level.

bigger than those calculated with the LSDA. The LDA + U calculation gives correct values for $LaSrMnO_4$.

Three-dimensional $LaMnO_3$ has A-type AF structure and Jahn–Teller distortion gives $3x^2 - r^2$ and $3y^2 - r^2$ orbital ordering. Recently, several theoretical calculations have shown that this orbital ordering is closely related to the in-plane FM state and the inter-plane AF state [8, 11]. However, two-dimensional $LaSrMnO_4$ has AF in-plane structure. Jahn–Teller distortion with elongation of the apex-oxygen-atom leads to $3z^2 - r^2$ orbital ordering and stabilizes the AF structure. In three-dimensional systems, this kind of Jahn–Teller distortion cannot occur, since the periodic arrangement of Mn and O atoms along the *c*-direction causes strong hybridization between $3z^2 - r^2$ orbitals of Mn and p_z orbitals of O_2 and it has no energy gap between the Mn e_g orbitals. It favours the FM state.

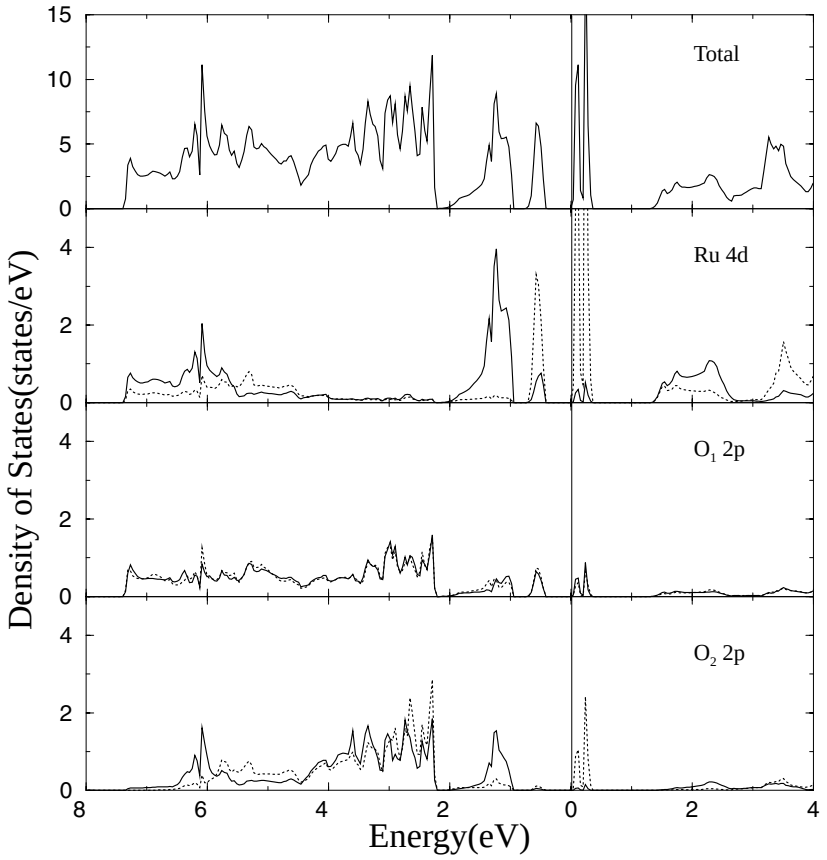

Figure 8. The total density of states and muffin-tin projected partial density of states of Ca_2RuO_4 obtained by LDA + U calculation. Solid and dotted lines in the second, third and fourth panels represent projected densities of states for up and down spins, respectively.

3.2. Ca_2RuO_4

Figure 7 and figure 8 show the LSDA-calculated total and partial densities of states and band structure, respectively Near the Fermi level, there are two t_{2g} levels (six bands) with up-spin and down-spin characters. In $LaSrMnO_4$, the exchange-splitting energy mJ (3 eV) is bigger than the crystal-field-splitting energy 10 Dq (1 eV). In Ca_2RuO_4, 10 Dq (3 eV) is bigger than mJ (0.8 eV) because of the difference between 3d and 4d orbital characters. The up-spin t_{2g} bands are fully occupied and the down-spin band is partially occupied. These t_{2g} levels are split into xy, yz, xz orbitals by the orthorhombic Jahn–Teller distortion of the Ru–O octahedron. The xz- and yz-related bands above the Fermi level are quite flat, because of the two-dimensional character (absence of c-direction Ru–O–Ru periodicity). Only the xy-related band is occupied and shows the orbital ordering nature. The charge-density plot of this band is shown in figure 9. However, LSDA calculation is not sufficient for describing the insulating nature, as for $LaSrMnO_4$. Ru oxide is also categorized as a strongly electron-correlated material. Figures 10 and 11 show the density of states and band structure calculated using the LDA + U method, respectively. These figures show the insulating gap and the orbital ordering nature.

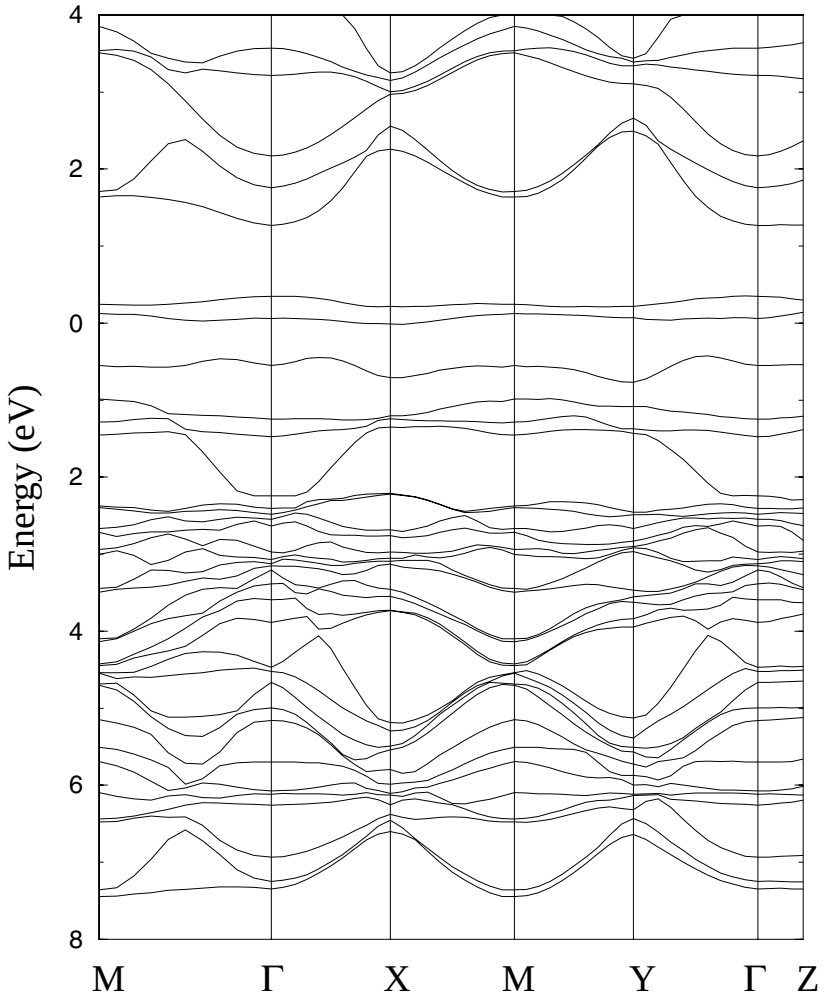

Figure 9. The energy band structure of Ca_2RuO_4 obtained by LDA + U calculation. Γ, X, M, Y and Z represent (0, 0, 0), (1/2, 0, 0), (1/2, 1/2, 0), (0, 1/2, 0), (0, 0, 1) k-points in the simple orthorhombic Brillouin zone, respectively. The conduction band minimum energy is chosen as 0 eV.

The LSDA-calculated total energy of the AF state is lower than those of the FM and PM states by 250 and 400 meV/cell, respectively. These energy differences are bigger than those for $LaSrMnO_4$. The Néel temperature calculated using equations (1) and (2) is 966 K. Although the calculated value is bigger than the experimentally observed value, $T_N = 110$ K, the temperature calculated in the molecular field approximation is close to the experimental value. The total energy difference calculated using the LDA + U approach is 160 meV bigger than the LSDA result.

The calculated magnetic moments inside the muffin-tin spheres are listed in table 2. The magnetic moments observed in experiments are dependent on the sample preparation, and vary from 0.4 to 1.3 μ_B [6, 17]. The value calculated using the LDA + U method, 1.32 μ_B, is quite similar to one experimental value.

Sr_2RuO_4 presents paramagnetic and superconducting behaviour. Since the Sr^{2+} ion is bigger than the Ca^{2+} ion, the Ru–O octahedron of $Sr2RuO_4$ shows a small tilt and rotation.

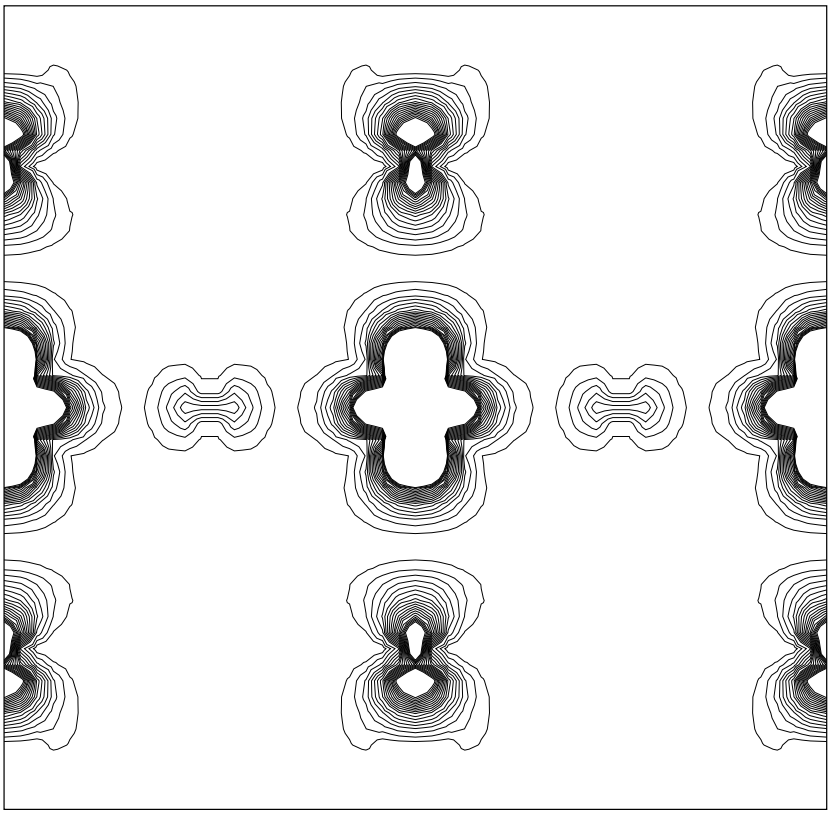

Figure 10. The charge-density plot in the (110) plane for $LaSrMnO_4$ near the Fermi level ($0 \leqslant E \leqslant -0.5$ eV).

Table 2. The magnetic moments (μ_B) and total energy (meV/cell). δE is the total-energy difference between the AF and FM energies ($E_{AF} - E_{FM}$).

	Magnetic moment			δE	
	AF (LSDA)	AF (LDA + U)	Experiment	LSDA	LDA + U
$LaSrMnO_4$	3.08	3.30	0.8[a]	−28	−248
$LaMnO_3$[b]	3.3	3.8	3.89	19.4	
Ca_2RuO_4	1.06	1.36	0.4[c], 1.3[d]	−250	−410

[a] Reference [7].
[b] Reference [10].
[c] Reference [6].
[d] Reference [17].

This gives strong hybridization between Ru and O atoms in Sr_2RuO_4 and increases the Ru bandwidth W. This prevents Sr_2RuO_4 from having an insulating nature. So, Sr_2RuO_4 favours paramagnetism and does not show Jahn–Teller distortion. Three-dimensional $CaRuO_3$ has a PM state and does not show Jahn–Teller distortion, even though it has small Ca^{2+} ions. There are two reasons for this. First, if $CaRuO_3$ has the same Jahn–Teller distortion as Ca_2RuO_4 (short Ru–O_2 and long Ru–O_1 distances), the bands related to Ru xz, yz orbitals are strongly

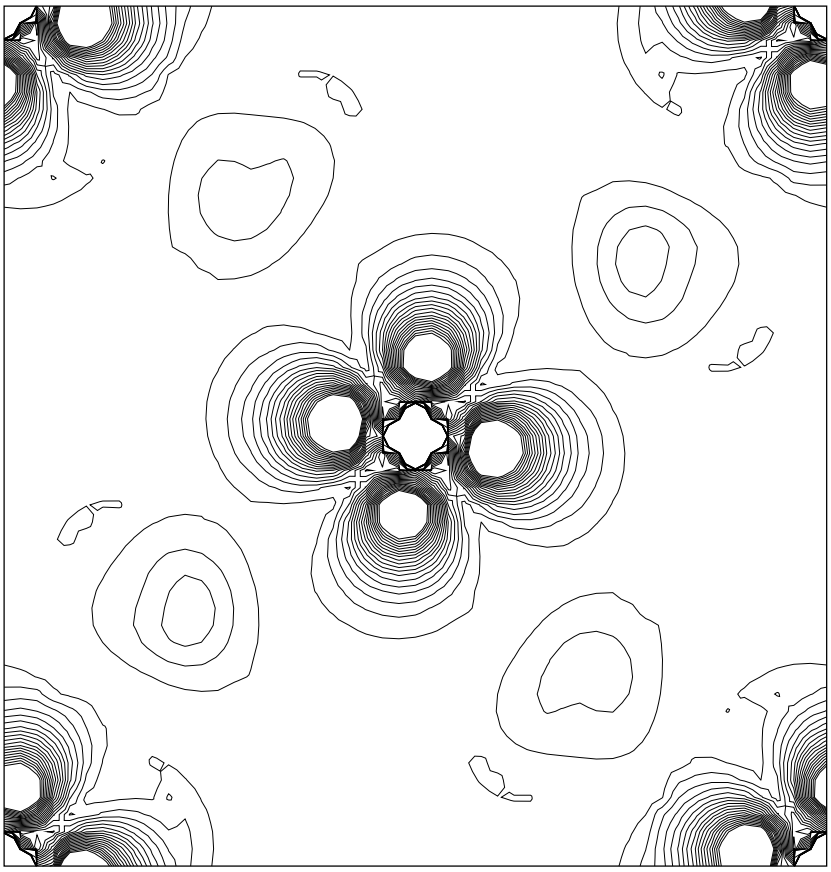

Figure 11. The charge-density plot in the (001) plane for Ca_2RuO_4 near the Fermi level ($0 \leqslant E \leqslant -0.5$ eV).

dispersive, because there is a periodic arrangement of Ru and O atoms along the c-direction (three-dimensionality). It does not show an insulating nature and the Jahn–Teller distortion is also unstable. Second, if it has $LaMnO_3$-type Jahn–Teller distortion (this gives $3x^2 - r^2$ and $3y^2 - r^2$ orbital ordering), $CaRuO_3$ does not show an insulating orbital ordering nature because the bands near the Fermi level are of t_{2g} character.

4. Conclusions

We performed first-principles electronic structure calculations for the 3d oxide $LaSrMnO_4$ and the 4d oxide Ca_2RuO_4 with layered perovskite structure. We investigated the electronic structures and magnetic structures using the LSDA and LDA + U methods. LSDA calculation for these materials is not sufficient for describing the insulating gap due to the Jahn–Teller distortion. In LDA + U calculations, the Jahn–Teller distortion and two-dimensional structure give an insulating gap, and $3z^2 - r^2$ and xy orbital ordering in $LaSrMnO_4$ and Ca_2RuO_4, respectively. The total-energy calculations show that the AF state is stable compared with the PM and FM states of these materials.

Acknowledgment

This work was accomplished with the aid of a Research Fund provided by the Korea Research Foundation, Support for Faculty Research Abroad.

References

[1] Moritomo Y, Asamitsu A, Kuwahara H and Tokura Y 1996 *Nature* **380** 141
[2] Maeno Y *et al* 1994 *Nature* **372** 532
[3] Nakatsuji S, Ikeda S and Maeno Y 1997 *J. Phys. Soc. Japan* **66** 1868
[4] Nakatsuji S and Maeno Y 2000 *Phys. Rev. Lett* **84** 2666
[5] Mazin I I and Singh D J 1997 *Phys. Rev.* B **56** 2556
[6] Braden M, Andre G, Nakatsuji S and Maeno Y 1998 *Phys. Rev.* B **58** 847
[7] Kawano S, Achiwa N, Kamegashira N and Aoki M 1988 *J. Physique Coll.* **C8** 829
[8] Solovyev I V and Terakura K 1998 *J Korean Phys. Soc.* **33** 375
[9] Liechtenstein A I, Anisimov V I and Zaanen J 1995 *Phys. Rev.* B **52** R5467
[10] Sawada H and Terakura K 1998 *Phys. Rev.* B **58** 6831
[11] Sawada H, Morikawa Y, Terakura K and Hamada N 1997 *Phys. Rev.* B **56** 12154
[12] Moritomo Y, Arima T and Tokura Y 1995 *J. Phys. Soc. Japan* **64** 4117
[13] Hohenberg P and Kohn W 1964 *Phys. Rev.* **136** B864
[14] Weinert M, Wimmer E and Freeman A J 1981 *Phys. Rev.* B **26** 4571
[15] Bouloux J, Soubeyroux J, Daoudi A and Flem G Le 1981 *Mater. Res. Bull.* **16** 855
[16] Moritomo Y *et al* 1995 *Phys. Rev.* B **51** 3297
[17] Cao G, McCall S, Shepard M, Crow J E and Guertin R P 1997 *Phys. Rev.* B **56** R2916